ARTICLE

Effect of Surface Capping with Poly(vinyl alcohol) on the Photocarrier Relaxation of ZnO Nanowires

Ashok Bera and Durga Basak*

Department of Solid State Physics, Indian Association for the Cultivation of Science, Jadavpur, Kolkata 700032, India

ABSTRACT The effect of surface capping with poly(vinyl alcohol) (PVA) on the photocarrier relaxation of the aqueous chemically grown ZnO nanowires (NWs) has been investigated. The decay in the photocurrent during steady ultraviolet illumination due to the photocarrier relaxation has been reduced in the capped NWs, as evidenced from a decrease in the photocurrent only by 12% of its maximum value under steady illumination for 15 min and a decrease in the photocurrent by 49% of its maximum value during the same interval of time in the as-grown NWs. The surface modification is confirmed from the FESEM, HRTEM, and FTIR results. The photoluminescence spectrum shows an enhanced ultraviolet emission and a reduced defect-related emission in the capped ZnO NWs compared to bare ZnO.

KEYWORDS: ZnO • PVA • surface capping • carrier relaxation

INTRODUCTION

Zinc oxide (ZnO) is one of the most important nanomaterials for nano-optoelectronics (1), light-emitting diodes (2), transistors (3), and nanopiezotronics (4) applications. With a band gap of 3.4 eV and an exciton binding energy of 60 meV, it has huge promise for ultraviolet (UV) photodetectors. The nanostructures of ZnO especially show very high conductivity under UV illumination (5, 6). It is well-known that two processes generally govern the UV photoconductivity in ZnO: (1) the surface-related process and (2) the bulk-related process. For the nanoscale materials, as the dimension decreases beyond a certain extent, it is possible that the surface approaches the bulk and the defects segregate on the surface, leaving a high-quality bulk devoid of defects and thereby producing a large difference in the properties. The interfacial property is very important, in such cases controlling the photoconductivity properties in the nanowires (NWs) due to the high surface-to-volume ratio. In the previous studies, we reported an anomalous photoconductivity that the photocurrent decreases even during steady UV illumination for aqueous chemically grown (ACG) ZnO NWs having diameters comparable to the corresponding Debye lengths (7, 8). It has been observed that this anomalous photoconductivity due to the carrier relaxation occurs through two processes: electron trapping by the surface states and recombination at the deep defect levels, which limits the growth of the photocurrent, thus reducing the photo-to-dark current ratio (η). Therefore, it is obvious that if the surface can be modified, the decay under steady illumination can be inhibited. There are quite a few reports on the surface capping of ZnO using inorganic as well as organic materials for different purposes. Shi et al. (9) and Yang et al. (10) have capped the surface by SnO_2 and poly(vinylpyrrolidone) (PVP), respectively, to enhance the photoluminescence (PL) properties of ZnO, while Lao et al. (11) have modified the NW surfaces by different UV-sensitive polymers to enhance the photoconductivity. Bouropoulos et al. (12) synthesized a ZnO−poly(vinyl alcohol) (PVA) nanocomposite, and Pauporte (13) synthesized PVA−ZnO composite thin films to study the electrical and optical properties. Wang et al. (14) used PVA to synthesize well-aligned ZnO nanorods to get more transmission. However, there is no report on the UV photoresponse properties of a ZnO−PVA composite. Because the surface capping is a way to modify the surface and thus the properties, which are largely affected by the surface interactions, it would be very interesting to investigate the UV photoconductivity of ZnO, especially the effect on the anomalous photoconductivity, by controlling the surface-related processes. Therefore, we have capped the surface of the ACG ZnO NWs with PVA to reduce the surface trapping of the carriers. The reason behind choosing PVA is that it is generally used to create a barrier for the O_2 (15, 16). Because adsorbed O_2 plays a major role in the photoconductivity of ZnO, PVA can reduce the adsorption of the O_2 molecules on the surface of ZnO. The photocurrent transients show that the maximum photocurrent value is larger for the capped ones compared to that of the as-grown NWs. The photocurrent of the PVA-capped ZnO NWs decreases only by 12% of its maximum value within 15 min under steady UV illumination, while the as-grown ZnO NWs show a decrease up to 49% of its maximum value for the same period of time. The PVA-capped ZnO NWs show

* To whom correspondence should be addressed. E-mail: sspdb@iacs.res.in. Fax: (91)-(33) 24732805.
Received for review June 19, 2009 and accepted August 2, 2009

DOI: 10.1021/am900422y
© 2009 American Chemical Society

Published on Web 08/13/2009

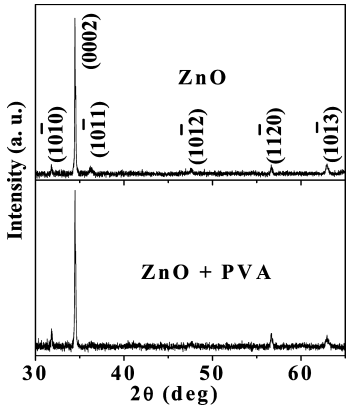

FIGURE 1. X-ray diffractograms of the as-grown and PVA-capped ZnO NWs.

a stronger UV emission peak in the PL spectrum compared to that of the as-grown ones.

EXPERIMENTAL SECTION

The quasi-vertical ZnO NWs grow on the quartz glass substrates following the ACG method as described elsewhere (7). In brief, we first deposited a ZnO seed layer by coating with a solution of zinc acetate and thermally decomposing it at 350 °C. Then, the NWs were grown by dipping the substrates with the seed layer in an equimolar mixture of $(CH_3COO)_2Zn \cdot 2H_2O$ and hexamethylenetetraamine $(CH_2)_6N_4$ (20 mM) in deionized water at 90 °C for 1 h. The substrates were then removed from the solution, rinsed in deionized water, and dried. For PVA capping, first 0.2 g of PVA (with molecular weight 115 000 g) was dissolved in 50 cm^3 of deionized water at 80 °C for 2 h and the mixture was kept at room temperature for 1 day to get a uniform solution. Then the previously prepared ZnO NWs were dipped into the solution at 50 °C for 1 h and then dried. The crystalline phase and morphology were confirmed by X-ray diffractometry (model Bruker D8), field-emission scanning electron microscopy (FESEM; JEOL model JSM-6700F), and high-resolution transmission electron microscopy (HRTEM; JEM model 2010). To confirm the capping of the NWs by PVA, Fourier transform infrared (FTIR) spectroscopy (Shimadzu model FTIR-8400) was done in the wavenumber region between 500 and 4000 cm^{-1}. For the photoresponse measurements, two gold electrodes (of 50 nm thickness) were thermally evaporated in the circular form of diameter 1 mm through a shadow mask at a separation of 3 mm on the top of ZnO NW arrays. The photocurrents were measured by illuminating the NWs with monochromatic light of wavelength 325 nm from a He−Cd laser (Kimmon Koha Co., Ltd., model KR1801C) of 100 mW power and using the Keithley picoammeter (model 2400) 3 V biasing condition. All of the experiments were done in ambient air at room temperature. The same He−Cd laser was used for optical excitation of the samples during PL measurement. A high-resolution spectrometer (Horiba Jobin Yvon model iHR 320) together with a photomultiplier tube was used to detect PL from the samples.

RESULTS AND DISCUSSION

X-ray diffractograms of the as-grown and PVA-capped ZnO NW arrays (Figure 1) show the presence of only the hexagonal wurtzite phase of ZnO, which indicates purity of the samples. The intensity of the (0002) peak is much higher than that of the other peaks, indicating that most of the NWs are aligned along the (0002) direction. The corresponding FESEM (inclined by 20°) images in Figure 2a,b showing the

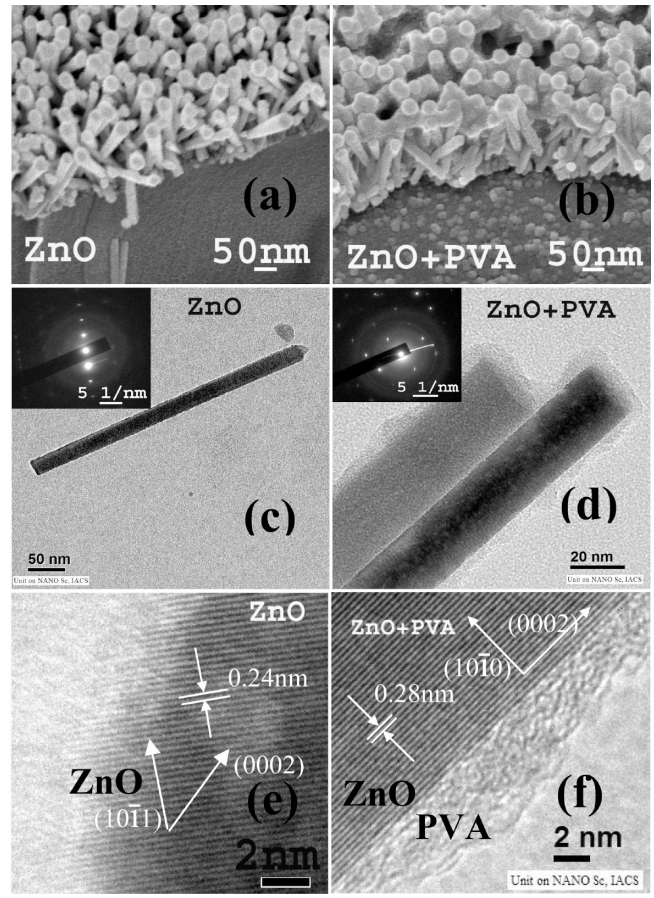

FIGURE 2. (a and b) FESEM, (c and d) TEM, and (e and f) HRTEM images of the as-grown and PVA-capped ZnO NWs. The insets in the TEM images show the corresponding SAED patterns.

morphologies support the X-ray diffractometry results. It is clear from the images that the NWs' surfaces are coated with PVA (thickened NWs) and PVA layers are present between the NW arrays in contrast to the thinner and well-separated as-grown NWs. The TEM images in Figure 2c,d show clearly the difference between the microstructure of the as-grown and PVA-capped NWs, supporting the FESEM results. The interplanar spacing in the fringe pattern of the HRTEM images also confirms the wurtzite structure of the ZnO NWs. PVA, on the other hand, does not show any fringe, as expected (Figure 2e,f). The corresponding selected-area electron diffraction (SAED) patterns (in the insets) confirm the hexagonal wurtzite phase of the ZnO NWs.

The presence of the PVA is further confirmed by recording the FTIR spectrum of the as-grown and PVA-capped ZnO NWs (Figure 3). The FTIR spectrum of the as-grown NWs shows a broad peak only at 3300−3600 cm^{-1} corresponding to the O−H mode of vibration, which arises because of the hydrogen-related defect states on the ACG ZnO NWs (17). The capped NWs, in addition to the above broad peak, show several peaks at 3359.77, 2941.24 and 1438.8, 1095.49, and 850 cm^{-1}, which are assigned to the alcoholic −OH−, $-CH_2$, −CO, and −C−CO groups (18), thereby confirming the presence of PVA on the NWs. Among the intrinsic defects, zinc vacancy (V_{Zn}), which can occur in both singly or doubly ionized states, V_{Zn}^{-1} or V_{Zn}^{-2}, is known to exist

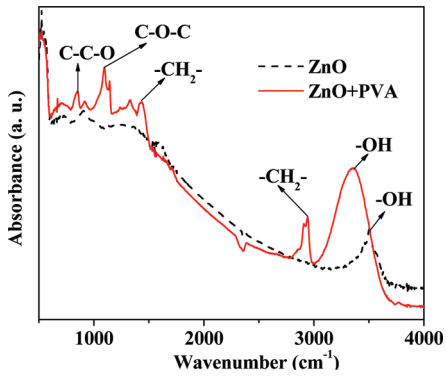

FIGURE 3. FTIR spectrum of the as-grown and PVA-capped ZnO NWs.

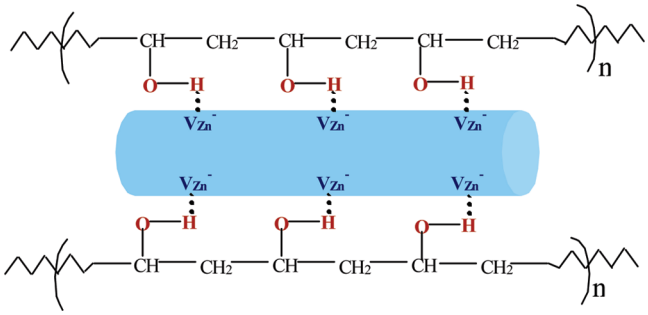

FIGURE 4. Surface interaction of ZnO NWs with PVA.

on the surface of the ACG ZnO NWs (19). PVA molecules, therefore, are most likely to get attached to the ZnO NW surface by forming a complex with the ionized V_{Zn} through weak electrostatic attraction, as shown in Figure 4. This is supported by the previous reports where PVA is shown to interact with the ZnO crystals (18, 20).

The schematic arrangement for the photocurrent measurements is shown in Figure 5a. In this case, the electrode contacts are Au/ZnO for ZnO NWs and Au/PVA/ZnO for PVA-capped NWs. All of the contacts show linear current–voltage (I–V) characteristics; i.e., all of the contacts are ohmic [Figure 5b]. Generally, these two different contacts should have different contact potentials, but when the sizes of the nanostructures are comparable to the space charge layer, surface depletion greatly affects the density and the mobility of the carriers in ZnO NWs rather than the contact potential (21). Because the PVA layer is very thin (around 3–5 nm), the carriers easily tunnel through the layer to the electrode. The dark current in the as-grown NWs is lower ($\approx 5.2 \times 10^{-10}$ A) compared to the value 1.35×10^{-9} A when the NW surfaces are capped with PVA. The photocurrent growth and decay were measured in ambient air by switching "on" and "off" the UV illumination (325 nm) for 15 min each (Figure 5c). On UV illumination, the photocurrent in the as-grown sample reaches a maximum value of 9.7×10^{-6} A, leading to the photo (I_{ph})-to-dark current (I_d) ratio I_{ph}/I_d of 1.8×10^4. In the case of the PVA-capped ZnO NWs, the photocurrent reaches a maximum value of 6.52×10^{-5} A, and thus I_{ph}/I_d becomes 4.8×10^4, which is more than double that of the as-grown sample. It is known that the surface-adsorbed O_2 and H_2O molecules largely affect the photoresponse of the NWs when the surface-to-volume ratio

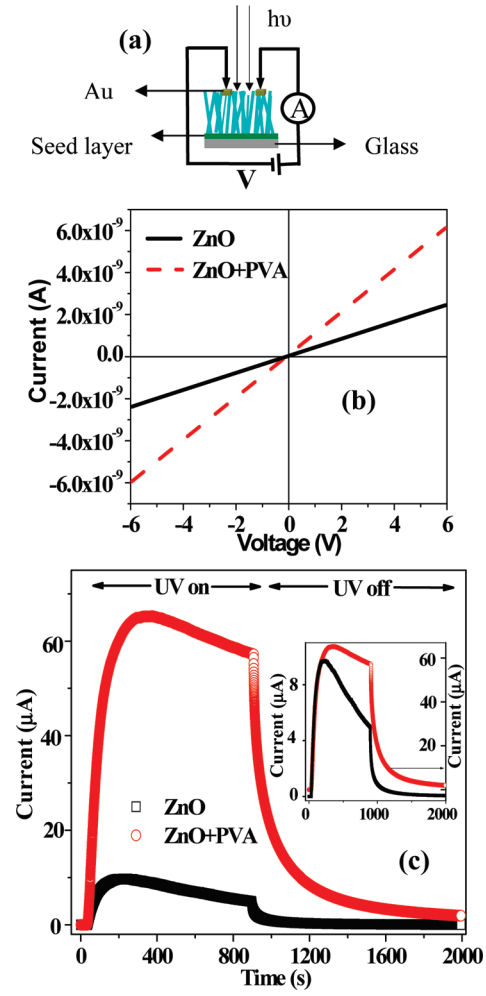

FIGURE 5. (a) Schematic diagram for the current measurement. (b) Dark I–V characteristic of the as-grown and PVA-capped ZnO NWs.(c) Photocurrent growth decay of the as-grown and PVA-capped ZnO NWs. The inset of the figure shows clearly the photocurrent decay under UV illumination.

is high (22). O_2 molecules are chemisorbed and physisorbed on the NW surfaces and get ionized as O_2^- by trapping electrons from the NWs, which results in the formation of a depletion layer, resulting in a band bending upward and leading to a barrier height for electrical conduction (23), as shown in Figure 6. On illumination, the photoexcited holes are generated and trapped by the adsorbed O_2^- through the surface electron–hole recombination, while the photoexcited unpaired electrons significantly increase the conductivity because of the increased lifetime (5). The PVA-capped NWs show higher dark current because of the smaller amount of adsorbed O_2, meaning fewer numbers of trapped carriers. Because of a higher photocurrent, the UV sensitivity of the capped NWs is more, even though the dark current is higher. Both types of NWs show a photocurrent decay under steady illumination, as reported earlier (7, 8). We have observed an interesting difference in these decay characteristics between the two types of NWs. The photocurrent of the as-grown ZnO NWs is up to 49% of its maximum value within 15 min of steady illumination while it is only 12% of its maximum value for the same period of time in PVA-capped NWs, which is clear from the inset in Figure 5c.

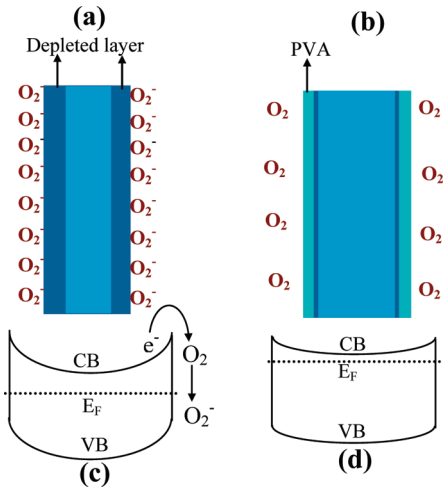

FIGURE 6. (a) Adsorption of O_2 molecules at the surfaces of the as-grown NWs leading to widening of the surface-depletion width. (b) Surface-depletion width, which is very small for the PVA-capped NWs. (c and d) Energy-band diagrams of the as-grown and PVA-capped ZnO NWs, respectively.

The photocurrent decay under steady illumination occurs through a two-electron process: electron capture by the surface states and electron recombination at the deep defect states (8). In brief, it can be explained as follows. When the UV illumination is on, the electron density in the conduction band increases because of trapping of the holes by the surface-adsorbed O_2^- as discussed earlier. Because the experiments were done in ambient air, the O_2 molecules are again adsorbed immediately after readsorption, reducing the electron density in the conduction band. Thus, there are always two competitive processes present in the photoconduction process. Apart from the electron trapping by the adsorbed O_2 molecules, the electrons are also recombined with the positively charged defect states Zn_i^{+2}, which is present because of the otherwise-formed $V_{Zn}-H_2O$ type of complex on the surface in the presence of adsorbed H_2O molecules instead of forming the $Zn_i^{+2}-V_{Zn}^{-2}$ defect (8). Because the recombination centers have a larger lifetime, the recombined electrons cannot be generated as fast as recombination occurs, resulting in a decrement in the photocurrent. However, this recombination part is not present or negligible when the NWs are heated thermally by the powerful UV radiation from the laser source. In that case, the surface trapping process becomes the dominating factor for decay of the photocurrent under steady illumination. From the above discussion, it is clear that although the photocarriers are generated during steady illumination, the current is not increased further after some time because of the simultaneous carrier relaxation process described above. Therefore, when the NWs are capped, due to surface modification, the further adsorption and desorption of O_2 molecules on the surface become negligible; this increases the photocurrent value, resulting in higher photosensitivity. It has been observed that the times taken for the 90% growth and decay of the maximum current are about 100 and 207 s, respectively, for the as-grown NWs. The values are 150 and 430 s, respectively, for the PVA-capped NWs. However, the slower growth and decay in the latter is due to the modification done by the capping because the adsorption and desorption of O_2 molecules make the photoresponse faster (22).

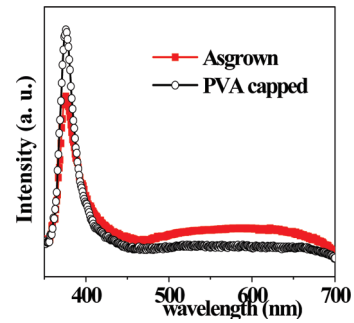

FIGURE 7. PL spectra of the as-grown and PVA-capped ZnO NWs.

The room temperature PL spectra of the as-grown and PVA-capped NWs show a very strong UV illumination peak at 376 nm and a weak broad emission in the visible region within 500−700 nm (Figure 7). The intensity of the UV emission peak for the PVA-capped NWs is much higher than that of the as-grown ones, while the intensity of the visible emission for the capped NWs is less than that of the as-grown NWs. The surface-adsorbed O_2 molecules cause the yellow-orange emission near 600 nm (7). When the NWs are capped with PVA, an almost absence of the adsorbed O_2 molecules on the surface of the NWs causes a less intense visible emission near 600 nm and hence results in the higher intense UV emission. Therefore, the PL results also provide support that there is surface modification in the PVA-capped NWs.

CONCLUSION

We have shown that the surfaces of the ACG ZnO NWs are modified significantly by capping with PVA. The photocurrent transients show that the photocurrent value is higher for the capped NWs and decreases only by 12% of its maximum value under steady illumination during 15 min, while the photocurrent value is lower in the as-grown ZnO NWs and shows a decrease up to 49% of its maximum value during the same period of time. The surface modification is evident from the enhanced UV emission and reduced defect-related emission in the PVA-capped NWs compared to that of the as-grown ones. The results demonstrate that the surface capping by PVA is useful in achieving a higher and relatively steady UV sensitivity in ZnO NWs.

Acknowledgment. This work is financially supported by the Council of Scientific and Industrial Research, New Delhi, India, via Project 03(1091)/07/EMR-II. The authors acknowledge the HRTEM facility created by the Department of Science and Technology, New Delhi, India.

REFERENCES AND NOTES

(1) Nakayama, Y.; Pauzauskie, P. J.; Radenovic, A.; Onorato, R. M.; Saykally, R. J.; Liphardt, J.; Yang, P. D. *Nature* **2007**, *447*, 1098.
(2) Guo, H.; Lin, Z.; Feng, Z.; Lin, L.; Zhou, J. *J. Phys. Chem. C* **2009**, DOI:10.1021/jp902607c.
(3) Lao, C. S.; Liu, J.; Gao, P. X.; Zhang, L. Y.; Davidovic, D.; Tummala, R.; Wang, Z. L. *Nano Lett.* **2006**, *6*, 263.
(4) Wang, Z. L. *Mater. Today* **2007**, *10*, 20.

(5) Soci, C.; Zhang, A.; Xiang, B.; Dayeh, S. A.; Aplin, D. P. R.; Park, J.; Bao, X. Y.; Lo, Y. H.; Wang, D. *Nano Lett.* **2007**, *7*, 1003.
(6) Jin, Y.; Wang, J.; Sun, B.; Blakesley, J. C.; Greenham, N. C. *Nano Lett.* **2008**, *8*, 1649.
(7) Bera, A.; Basak, D. *Appl. Phys. Lett.* **2008**, *93*, 053102.
(8) Bera, A.; Basak, D. *Appl. Phys. Lett.* **2009**, *94*, 163119.
(9) Shi, L.; Xu, Y.; Hark, S.; Liu, Y.; Wang, S.; Peng, L.; Wong, K.; Li, Q. *Nano Lett.* **2007**, *7*, 3559.
(10) Yang, C. L.; Wang, J. N.; Ge, W. K.; Guo, L.; Yang, S. H.; Shen, D. Z. *J. Appl. Phys.* **2001**, *90*, 4489.
(11) Lao, C. S.; Park, M. C.; Kuang, Q.; Deng, Y.; Sood, A. K.; Polla, D. L.; Wang, Z. L. *J. Am. Chem. Soc.* **2007**, *129*, 12096.
(12) Bouropoulos, N.; Psarras, G. C.; Moustakas, N.; Chrissanthopoulos, A.; Baskoutas, S. *Phys. Status Solidi A* **2008**, *8*, 2033.
(13) Pauporte, T. *Cryst. Growth Des.* **2007**, *7*, 2310.
(14) Wang, Z.; Huang, B.; Qin, X.; Zhang, X.; Wang, P.; Wei, J.; Zhan, J.; Jing, X.; Liu, H.; Xu, Z.; Cheng, H.; Wang, X.; Zheng, Z. *Mater. Lett.* **2009**, *63*, 130.
(15) Miller, K. S.; Krochta, J. M. *Trends Food Sci. Technol.* **1997**, *8*, 228.
(16) Lange, J.; Wyser, Y. *Packing Sci. Technol.* **2003**, *16*, 149.
(17) Wahab, R.; Ansari, S. G.; Kim, Y. S.; Song, M.; Shin, H. S. *Appl. Surf. Sci.* **2009**, *255*, 4891.
(18) Sui, X. M.; Shao, C. L.; Liu, Y. C. *Appl. Phys. Lett.* **2005**, *87*, 113115.
(19) Tam, K. H.; Cheung, C. K.; Leung, Y. H.; Djurisic, A. B.; Ling, C. C.; Beling, C. D.; Fung, S.; Kwok, W. M. W.; Chan, K.; Phillips, D. L.; Ding, L.; Ge, W. K. *J. Phys. Chem. B* **2006**, *110*, 20865.
(20) Kumar, R. V.; Elgamiel, R.; Koltypin, Y.; Norwig, J.; Gedanken, A. *J. Cryst. Growth* **2003**, *250*, 409.
(21) Li, C. C.; Du, Z. F.; Li, L. M.; Yu, H. C.; Wan, Q.; Wang, T. H. *Appl. Phys. Lett.* **2007**, *91*, 032101.
(22) Li, H. Q.; Gao, T.; Wang, Y. G.; Wang, T. H. *Appl. Phys. Lett.* **2005**, *86*, 123117.
(23) Feng, P.; Wan, Q.; Wang, T. H. *Appl. Phys. Lett.* **2005**, *87*, 213111.

AM900422Y